Supporting Information

Inorganic-organic hybrid nano material with core-shell structure constructed by Mn-BTC and $Ag_5[BW_{12}O_{40}]$ for supercapacitors and photocatalytic dye degradation

Shi Caihong[a], Kang Ning[a], Wang Chunmei[a], Yu Kai[ab]*, Lv Jinghua[a], Wang Chunxiao[a], Zhou Baibin[ab]*

1. Experimental section

1.1. Material and characterization methods

All reagents are commercially available and used as received without further purification. Fourier transform infrared (FTIR) spectra of compound was carried out on a Nicolet-360 spectrophotometer in the range of 400-4000 cm^{-1} using KBr particles. Use Hitachi SU-70 scanning electron microscope (SEM) produced by Hitachi to analyze the morphology and content. The transmission electron microscopy (TEM) images were performed on aultrahigh resolution scanning electron microscope (JEOL2010, Japan). Thermogravimetric analysis (TGA) is a PerkinElmer Diamond 6300 differential thermal analyzer produced in the United States, with α-Al_2O_3 as the reference material, using a platinum crucible, the heating rate is 10°C min^{-1}, and the heating is 25°C to 800°C, N_2 protects the atmosphere of the system. X-ray photoelectron spectroscopy (XPS) test equipment comes from Shimadzu Corporation, Japan, model is Axis Ultra DLD, after analyzing the element valence state and distribution of the sample. The specific surface area (BET) test instrument comes from the United States Kangta company, the model is Nova 2000E specific surface area analyzer. Powder X-ray diffraction (XRD, BRUKER D8) using Cu Kα radiation (λ= 0.154 nm) was employed to identify the crystalline phase of the material and the range of 2θ from 20-80°. Sampling and analysis of the sample via the Varian Cary 500 UV-Vis-NIR spectrometer. Photoluminescence (PL) spectra of the samples were measured with a Hitachi F-4500 fluorescence spectrophotometer at room temperature using He–Cd laser as an excitation light source. The excitation wavelength was 325 nm.

1.2. Synthesis of $K_5BW_{12}O_{40}•15H_2O$

Refer to the literature,[1] the synthesis of was slightly modified. The typical method is: 40 g $Na_2W_{12}O_{40}·2H_2O$ and 3 g H_3BO_3 were dissolved in 60 mL distilled water. Adjusted pH to 6 with 6 M HCl solution and boiled for 2 h under magnetic stirring. Filtered to remove impurities. After that, the pH of the filtrate obtained was modulated 2 with 6 M HCl solution and 80 g KCl was added. At this time, precipitation was generated in the solution. The solution was filtered, washed with ether to precipitation and dried to obtain 23.2 g product. It was verified that the IR spectra are basically consistent with the literature.

1.3. Synthesis of $Ag_5[BW_{12}O_{40}]$

$AgNO_3$ (0.24 g, 1.142 mmol) and $K_5[BW_{12}O_{40}]·15H_2O$ (0.2800 g, 0.0918 mmol) were successively dissolved in

10 mL distilled water. After the evaporative crystallization, filtered and washed, the gray powdery sample of $Ag_5[BW_{12}O_{40}]$ was obtained by drying it in 60°C over for 1 day.

1.4. Electrode preparation

The active substance was prepared by mixing acetylene black with powder at a mass ratio of 1:4, and then dried in 50°C oven after 50 min of ultrasonic. 5mg of the active substance was dissolved in 150 μL ethanol solution (ethanol : water =1:3) and dispersed ultrasonic for 40 min to prepare slurry. The nickel foam (NF) was cut to a size of 1×3 cm^2. Apply paste to the position of 1×1 cm^2 nickel foam. Dry in 50°C oven for 4 h to remove solvent. The nickel foam was laminated with a press at a pressure of 2 MPa. The mass difference before and after the nickel foam was attributed to the active substance loading.

1.5. Electrochemical measurement

At room temperature, CHI 660E electrochemical workstation (Shanghai Chenhua Instrument Co. Ltd.) was connected with a computer, 1 M Na_2SO_4 solution was used as electrolyte. The electrochemical properties of the synthesized compounds were tested by cyclic voltammetry (CV), galvanostatic charge/discharge (GCD) method, and electrochemical impedance spectroscopy (EIS). In the three-electrode system, nickel foam uses as the working electrode, Pt wire as the counter electrode, and Ag/AgCl (3 mol L^{-1} KCl) electrode as the reference electrode. The two-electrode system uses nickel foam electrode material as a positive and negative electrode. The weight of the two nickel foam electrodes have approximately the same weight.

1.6. Photocatalytic measurement

Ultraviolet (UV) degradation experiment was carried out on 15 mg L^{-1} MB, RhB, and MO three dye solutions. First, the optical absorption properties of the three compounds were tested separately. Under light avoidance conditions, 40 mg of compounds were added to 80 mL of three dyes and stirred for 50 min. 3 mL of mixture was removed every 10 min and put into a centrifuge, and the liquid supernatant was removed to measure its absorbance. The photocatalytic degradation properties of the three compounds were then tested. 40 mg of the compound was placed in 80 mL dye solution, adsorbed and stirred for 30 min in a dark room to ensure that the catalyst reached the adsorption/desorption balance. 3 mL of the solution was taken. The rest of the solution, under stirring, illuminated with a mercury lamp (125 W, 365 nm). Every about 20 minutes apart, 3 mL of solution was taken, centrifuged, and the supernatant was taken for UV spectrum to calculate the degradation rate. Simultaneously conduct five photocatalytic cycle tests.

1.7. Computational formula

The specific capacitance of the three electrodes system is calculated as follow:[2]

$C_s = I \times \Delta t / (m \times \Delta V)$ Equation(S1)

Where C_s $(F \cdot g^{-1})$is specific capacitance, I (A) is the discharge current, Δt (s) is the discharge time, ΔV (V) is the voltage window and m (g) is the load of the active material in the electrode.

The formula for calculating the specific capacitance of two electrodes:[3]

$C = 2I \times \Delta t / (m \times \Delta V)$ Equation(S2)

where I is the current density (A), Δt is designates the discharge time(s), m signifies mass of both the

electrodes (g) and ΔV represents voltage window (V), respectively. The energy density (E, $\mathrm{Wh \cdot kg^{-1}}$) and power density ($P$, $\mathrm{W \cdot kg^{-1}}$) calculation formulas are as follows:

$E = C\Delta V^2/7.2$ Equation(S3)

$P = E \times 3600/\Delta t$ Equation(S4)

EIS tests 5 mV AC voltage as the signal source, and its frequency range is 10^{-2}-10^{5} Hz.

2. Results and Discussion

2.1. TG

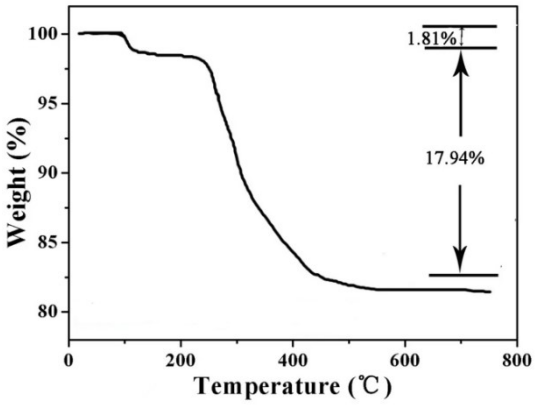

Fig S1. TG curve of Mn-BTC@$Ag_5[BW_{12}O_{40}]$

2.2. EDX

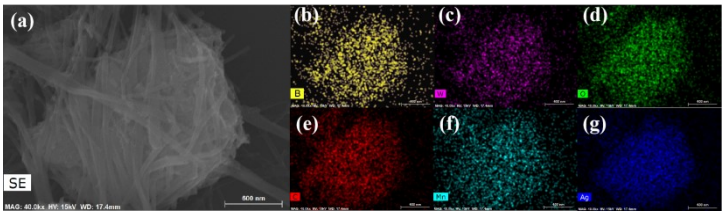

Fig S2. (a)-(g) EDX mapping of Mn-BTC@$Ag_5[BW_{12}O_{40}]$

2.2. BET

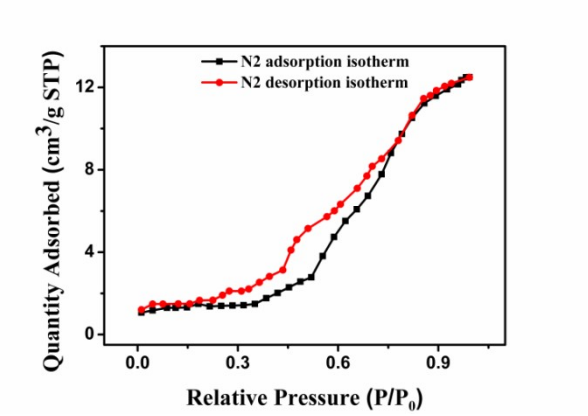

Fig S3. N_2 absorption-desorption isotherm of Mn-BTC@$Ag_5[BW_{12}O_{40}]$

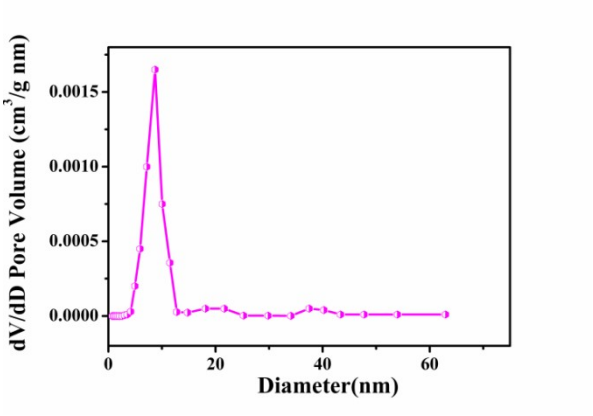

Fig S4. Pore size distribution of Mn-BTC@$Ag_5[BW_{12}O_{40}]$

2.3. XPS

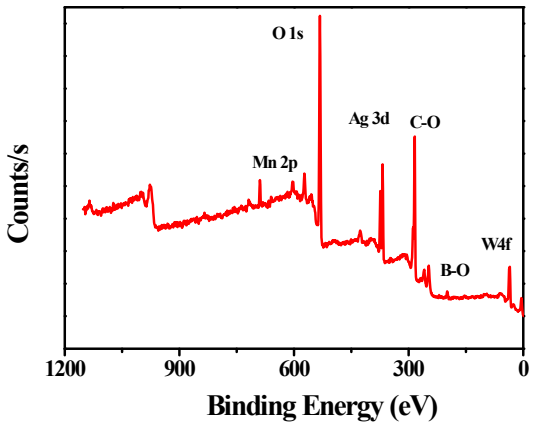

Fig S5. XPS spectra of Mn-BTC@$Ag_5[BW_{12}O_{40}]$

2.4. Electrochemical properties

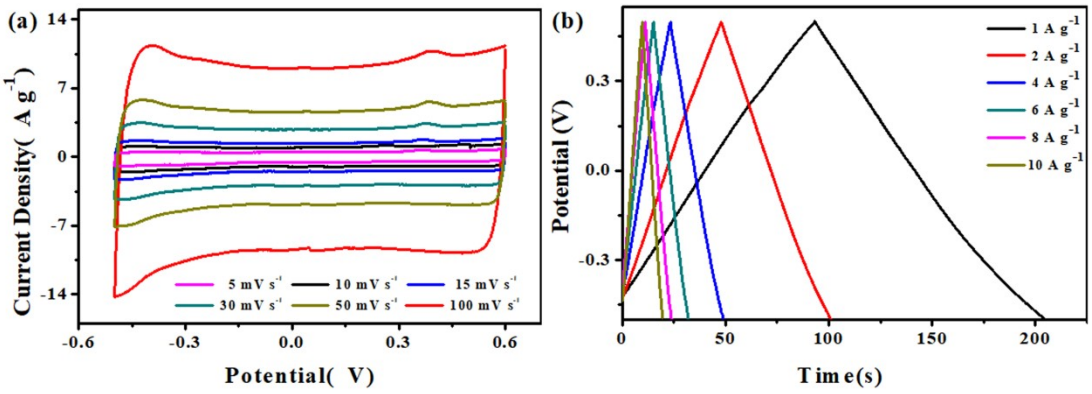

Fig S6. (a) CV curves at different scan rates and (b) GCD curves of $Ag_5[BW_{12}O_{40}]$-NF

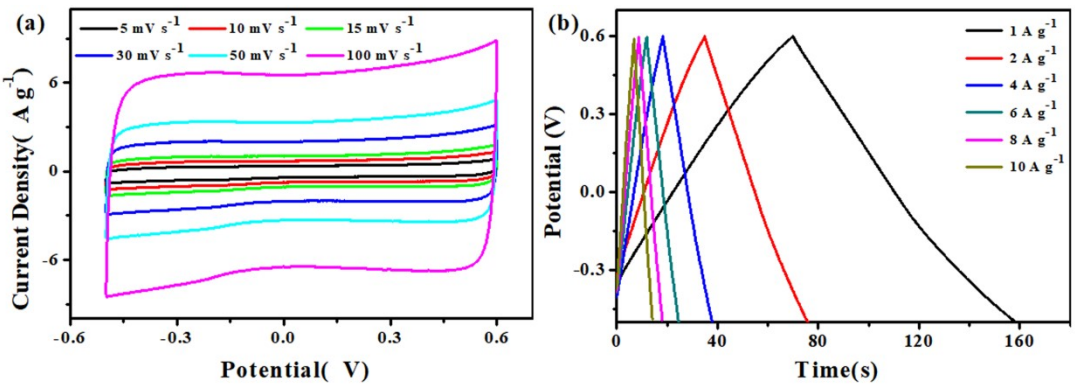

Fig S7. (a) CV curves at different scan rates and (b) GCD curves of Mn-BTC-NF

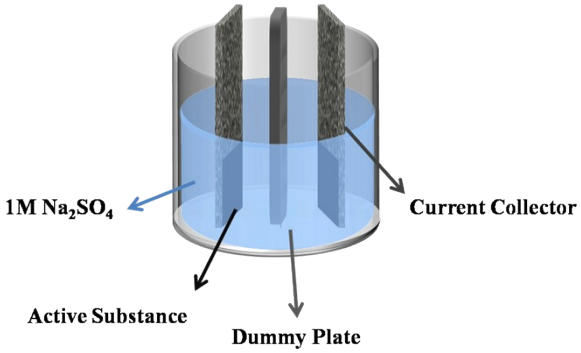

Fig S8. A simulation of a symmetric SSC system.

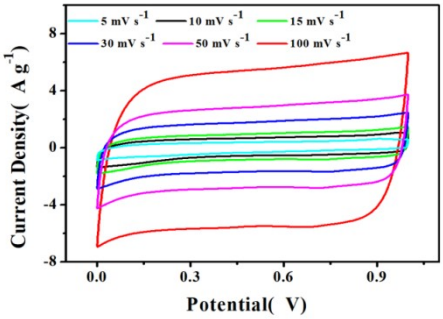

Fig S9. CV curves at different scan rates of 5–100 mV s^{-1} for SSC

2.5. Photocatalytic of Mn-BTC@$Ag_5[BW_{12}O_{40}]$

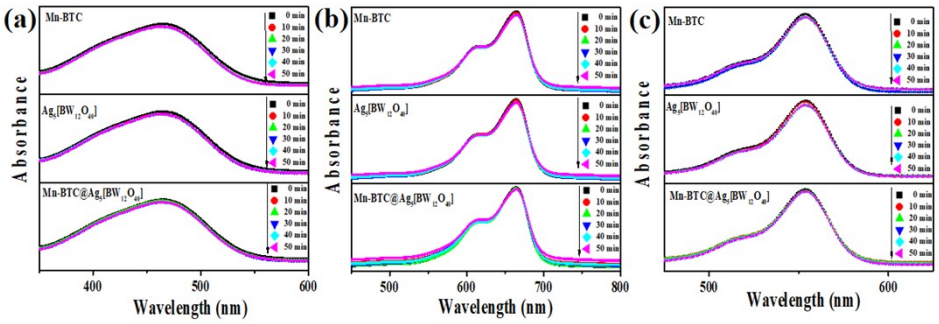

Fig S10. (a-c) The absorption spectra of MO, MB, RhB with three compounds in the dark

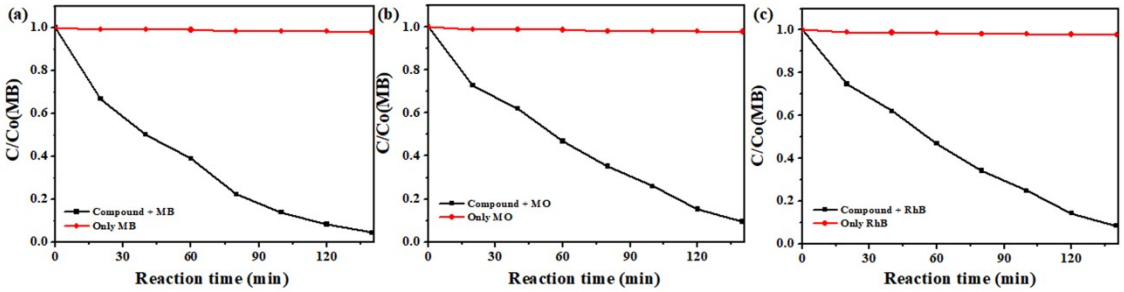

Fig S11. (a-c) The conversion rate of MB, MO, RhB with the same reaction time of phlocatalyst and no catalyst

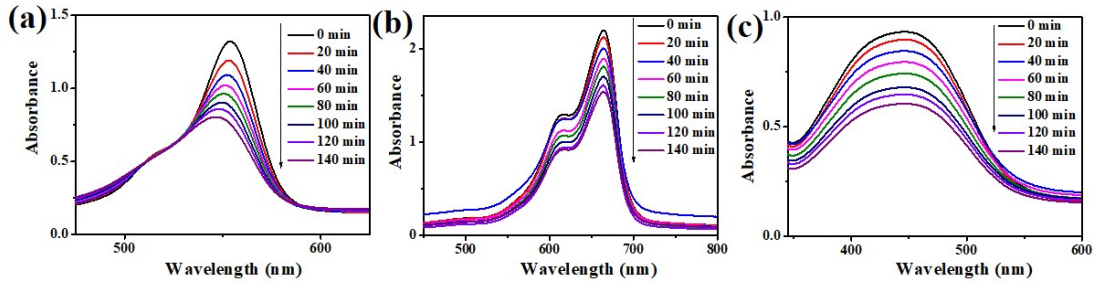

Fig S12. (a-c) The absorption spectra of RhB, MB, MO with $Ag_5[BW_{12}O_{40}]$ during the decomposition reaction under UV irradiation

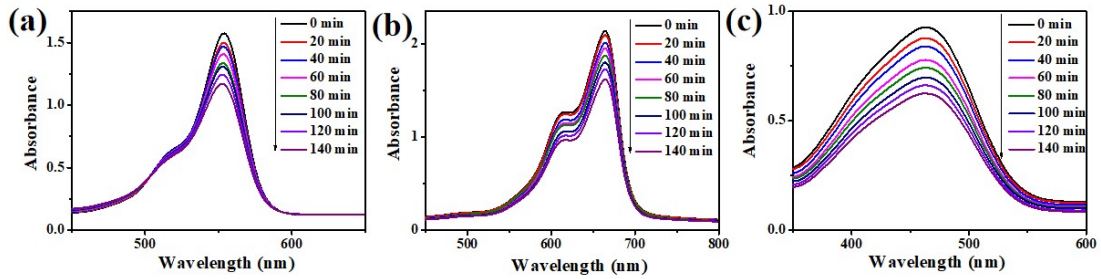

Fig S13. (a-c) The absorption spectra of RhB, MB, MO with Mn-BTC during the decomposition reaction under UV irradiation

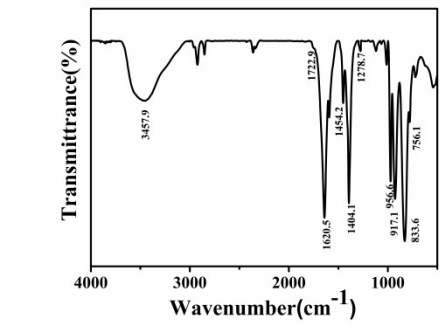

Fig S14. The IR of Mn-BTC@$Ag_5[BW_{12}O_{40}]$ after five cycles

Table S1. Comparison of the properties of the Keggin POMs-based materials with several published supercapacitors

	materials	specific capacitance	cycling stability	current collector	Ref.
1	PAni/$H_3PMo_{12}O_{40}$	120 F g^{-1} (0.4 A g^{-1})	70% (1000 cycles)	Rigid graphite plate	4
2	$H_3PMo_{12}O_{40}$/MWCNT	38 F g^{-1} (1 A g^{-1})		porous glassy fibrous paper	5
3	AC/$PMo_{12}O_{40}$	136 F g^{-1} (2 A g^{-1})	91% (8000cycles)	glassy carbon	6
4	RGO/ $PMo_{12}O_{40}$	51.2 F g^{-1} (5 mV s^{-1})	95% (5000 cycles)	commercial Flexible carbon cloth	7
5	PMo_{12}–$XW_xO_{40}^{3-}$	140 F g^{-1} (10 A g^{-1})	94.6% (1700cycles)	glassy carbon	8
6	$[Ag_5(brtmb)_4][VW_{10}V_2O_{40}]$	206 F g^{-1} (110 A g^{-1})	81.7% (1000 cycles)	glassy carbon	9
7	rGO-PMo_{12}‖rGO-PW_{12}	110 mF cm^{-2} (2 mA cm^{-2})	95% (2000 cycles)	carbon cloth	10
8	$[Cu^{I}(btx)]_4[SiW_{12}O_{40}]$	110.3 F g^{-1} (3 A g^{-1})	87% (1000 cycles)	glassy carbon	11
9	$[\{Cu^{I}_6(btx)_7(H_2O)_{12}\}H_4(W_{12}O_{40})_2]\cdot 12H_2O$	50.0 F g^{-1} (3 A g^{-1})	87.5% (1000 cycles)	glassy carbon	10
10	$[H(C_{10}H_{10}N_2)Cu_2][PW_{12}O_{40}]$	153.43 F g^{-1} (1 A g^{-1})	18.2% (500 cycles)	glassy carbon	12
11	AC/$PMo_{12}O_{40}$	183 F g^{-1} (2 A g^{-1})	98% (3000 cycles)	graphite rods	13
12	mPPy@GO-PMo_{12}	115 mF cm^{-2} (1 mV s^{-1})	80% (2000 cycles)	glassy carbon	14
13	$[Ag_5(C_2H_2N_3)_6][H_5?SiMO_{12}O_{40}]$@15%GO	230.2 F g^{-1} (0.5 A g^{-1})	92.7% (1000 cycles)	glassy carbon	15
14	$[Ag_5(C_2H_2N_3)_6][H_5?SiMo_{12}O_{40}]$	155.0 F g^{-1} (0.5 A g^{-1})	78.5% (1000 cycles)	glassy carbon	15
15	$[Ag_5(C_2H_2N_3)_6][H_5?SiW_{12}O_{40}]$	29.8 F g^{-1} (0.5 A g^{-1})	78.3% (1000 cycles)	glassy carbon	15
16	$[Cu^{I}H_2(C_{12}H_{12}N_6)(PMo_{12}O_{40})]\cdot[(C_6H_{15}N)(H_2O)_2]$	249 F g^{-1} (3 A g^{-1})	93.5% (1000 cycles)	glassy carbon	16
17	$[Cu^{II}_2(C_{12}H_{12}N_6)_4(PMo^{VI}_9Mo^{V}_3O_{39})]$	154.5 F g^{-1} (3 A g^{-1})	91.1% (1000 cycles)	glassy carbon	16
18	$[Cu^{I}_4H_2(btx)_5(PMo_{12}O_{40})]\cdot 2H_2O$	237 F g^{-1} (2 A g^{-1})	92.5% (1000 cycles)	glassy carbon	17
19	$[Cu^{I}_4H_2(btx)_5(PW_{12}O_{40})_2]\cdot 2H_2O$	100 F g^{-1} (2 A g^{-1})	90% (1000cycles)	glassy carbon	17

20	$[Cu^{II}Cu^{I}_3(H_2O)_2(btx)_5(PW^{VI}_{10}W^{V}_2O_{40})]\cdot 2H_2O$	82.1 F g^{-1} (2 A g^{-1})	100% (1000cycles)	glassy carbon	17
21	$[Cu^{I}_6(btx)_6(PW^{VI}_9W^{V}_3O_4]\cdot 2H_2O$	76.4 F g^{-1} (2 A g^{-1})	100% (1000cycles)	glassy carbon	17
22	$[Cu^{II}Cu^{I}_3(btx)_5(SiMo^{VI}_{11}Mo^{V}O_{40})]\cdot 4H_2O$	138.4 F g^{-1} (2 A g^{-1})	97% (1000cycles)	glassy carbon	17
23	$[Ag_{10}(trz)_8][HVW_{12}O_{40}]$	93.5 F g^{-1} (1.5 A g^{-1})	59.2% (750 cycles)	glassy carbon	18
24	$[Ag_{10}(trz)_6][SiW_{12}O_{40}]$	47.8 F g^{-1} (1.5 A g^{-1})	90.9% (1000 cycles)	glassy carbon	18
25	$[Ag(trz)][Ag_{12}(trz)_9][H_2BW_{12}O_{40}]$	42.9 F g^{-1} (1.5 A g^{-1})	86.5% (1000 cycles)	glassy carbon	18
26	$[Mn_2(BTC)_{4/3}(H_2O)_6]_6$ $[K_8(SiW_{10}Mn_2C_{l4}O_{36})]$	211.0 F g^{-1} (1 A g^{-1})	96.0% (5000 cycles)	nickel foam	19
27	AC/TEAPW$_{12}$	82 F g^{-1} (0.5 A g^{-1})	93% (10000 cycles)	aluminum foil	20
28	$H_3PW^{VI}_{12}O_{40}\cdot(BPE)_{2.5}\cdot 3H_2O$	49.2 F g^{-1} (2 A g^{-1})	80.4% (1000 cycles)	glassy carbon	21
29	$H_3PMo^{VI}_{12}O_{40}\cdot(BPE)_{2.5}\cdot 3H_2O$	137.5 F g^{-1} (2 A g^{-1})	92.0% (1000 cycles)	glassy carbon	21
30	$[HPMo^{VI}_9Mo^{V}_3O_{40}]Cu^{I}_5[4\text{- atrz}]_6\cdot H_2O$	231.7 F g^{-1} (1 A g^{-1})	88.2% (1000 cycles)	glassy carbon	22
31	$[HPW^{VI}_9W^{V}_3O_{40}]Cu^{I}_5[4\text{- atrz}]_6$	147.5 F g^{-1} (1 A g^{-1})	95.3% (1000 cycles)	glassy carbon	22
32	$[H_2SiMo^{VI}_9Mo^{V}_3O_{40}]Cu^{I}_5[4\text{-atrz}]_6\cdot H_2O$	232.5 F g^{-1} (1 A g^{-1})	98.8% (1000 cycles)	glassy carbon	22
33	$L_{0.5}[Cu_2L_{3.5}(SiW_{12}O_{40})]$	159.2 F g^{-1} (3 A g^{-1})		glassy carbon	23
34	PW$_{12}$@MIL-101 /PPy-0.15	1124 mF·cm^{-2} (0.5 mA·cm^{-2})		nickel foam	24
35	PW$_{12}$@MIL-101	158 mF·cm^{-2} (0.5 mA·cm^{-2})		nickel foam	24
36	$H[Cu_2(4\text{-Hdpye})_2(PMo_{12}O_{40})(H_2O)_4]\cdot 2H_2O$	196.6 F g^{-1} (0.5 A g^{-1})		carbon cloth	25
37	$[Co(H_2Ptep)(HPtep)(H_2O)_2(PW_{11}CoO_{39})]\cdot 4.5H_2O$	212 F g^{-1} (1 A g^{-1})	90.2% (1000 cycles)	glassy carbon	26
38	$[Co(H_2Ptpi)_2(HPtpi)_2(SiMo_{12}O_{40)2}]\cdot 2H_2O$	202 F g^{-1} (1 A g^{-1})	85.8% (1000 cycles)	glassy carbon	26
39	$\{Zn_2(DEP)_2(H_2O)_6[H_2(TeMo_6O_{24})]\}$	412.77 F g^{-1} (1 A g^{-1})	81.5% (1000 cycles)	glassy carbon	27
40	$\{Co(DEP)_2(H_2O)_2[H_2(\gamma\text{-}Mo_8O_{26})]\}\cdot 11H_2O$	580 F g^{-1} (1 A g^{-1})	73.3% (1000 cycles)	glassy carbon	27
41	$\{Cu(DEP)[(H_2\beta\text{-}Mo_8O_{26})_{0.5}]\}$	823.09 F g^{-1} (1 A g^{-1})	79.4% (1000 cycles)	glassy carbon	27

42	$[Ni_7(1,2,4\text{-tri})_{12}(H_2O)_{10}][HPMo_{12}O_{40}]\cdot 10H_2O$	815.6 F g^{-1} (1 A g^{-1})	93.8% (6000 cycles)	glassy carbon	28
43	$[Cu_2(Cmt)_2(OH)Cl(\beta\text{-}Mo_8O_{26})_{0.5}]$	378 F g^{-1} (1 A g^{-1})	75% (1000 cycles)	glassy carbon	29
44	$[Cu(H_2O)_3(H_{3/2}Tpm)_2](HTpm)(PMo_{12}O_{40})_2\cdot 4H_2O$	1618 F g^{-1} (1 A g^{-1})	83.8% (1000 cycles)	glassy carbon	29
45	Mn-BTC@$Ag_5[BW_{12}O_{40}]$	198.09 F g^{-1} (1 A g^{-1})	94.4% (5000 cycles)	nickel foam	This work

Notes and references

1. C. R. Deltcheff, M. Fournier, R. Franck, R. Thouvenot, *Inorg. Chem.*, 1983, **22**, 207-216.
2. L. X. Zheng, C. D. Wang, Y. C. Dong, H. D. Bian, T. F. Hung, J. Lu, Y. Y. Li, *Appl. Surf. Sci.*, 2016, **362**, 399-405.
3. L. G. Gong, X. X. Qi, K.Yu, J. Q. Gao, B. B. Zhou, G. Y. Yang, *J. Mater. Chem.*, 2020, **8**, 5709-5720.
4. A. K. C. Gallegos, M. L. Cantú, N. C. Pastor, P. G. Romero, *Adv. Funct. Mater.*, 2005, **15**, 1125-1133.
5. M. Skunik, M. Chojak, I. A. Rutkowska, P. J. Kulesza, *Electrochim. Acta*, 2008, **53** 3862-3869.
6. V. Ruiz, J. Suárez-Guevara, P. Gomez-Romero, *Electrochem. Commun.*, 2014, **24** 35-38.
7. D. P. Dubal, J. Suarez-Guevara, D. Tonti, E. Enciso, P. Gomez-Romero, *J. Mater. Chem.*, 2015, **3**, 23483-23492.
8. Y. H. Ding, J. Peng, H. Y. Lu, Y. Yuan, *RSC Adv.*, 2016, **6**, 81085-81091.
9. G. N. Wang, T. T. Chen, X. M. Wang, H. Y. Ma, H. J. Pang, *Eur. J. Inorg. Chem.*, 2017, **2017**, 5350-5355.
10. D. F. Chai, Y. Hou, K. P. O'Halloran, H. J. Pang, H. Y. Ma, G. N. Wang, X. M. Wang, *ChemElectroChem*, 2018, **5**, 3443-3450.
11. H. N. Wang, M. Zhang, A. M. Zhang, F. C. Shen, X. K. Wang, S. N. Sun, Y. J. Chen, Y. Q. Lan, *ACS Appl. Mater. Interfaces*, 2018, **10**, 32265-32270.
12. S. Roy, V. Vemuri, S. Maiti, K. S. Manoj, U. Subbarao, S. C. Peter, *Inorg. Chem.*, 2018, **57**, 12078-12092.
13. J. Suarez-Guevara, V. Ruiz, P. Gomez-Romero, *J. Mater.Chem.*, 2014, **2**, 1014-1021.
14. J. Q. Qin, F. Zhou, H. Xiao, R. Y. Ren, Z. S. Wu, *Sci. China Mater.*, 2018, **61**, 233-242.
15. Y. Hou, D. F. Chai, B. N. Li, H. J. Pang, H. Y. Ma, X. M. Wang, L. C. Tan, *ACS Appl. Mater. Interfaces*, 2019, **11**, 20845-20853.
16. D. F. Chai, J. J. Xin, B. N. Li, H. J. Pang, H. Y. Ma, K. Q. Li, B. X. Xiao, X. M. Wanga, L. C. Tana, *Dalton Trans.*, 219, **48**, 13026-13033.
17. D. F. Chai, C. J. G. García, B. Lia, H. Panga, H. Y. Ma, X. M. Wang, L. C. Tan, *Chem. Eng. J.*, 2019, **373**, 587-597.
18. Y. Hou, H. J. Pang, C. J. Gómez-García, H. Y. Ma, X. M. Wang, L. C. Tan, *Inorg. Chem.*, 2019, **58**, 16028-16039.
19. Z. W. Zheng, X. Y. Zhao, L. G. Gong, C. X. Wang, C. M. Wang, K. Yu, B. B. Zhou, *J. Solid State Chem.*, 2020, **288**, 121409.
20. J. J. Zhu, R. B. Vilaua, P. G. Romero, *Electrochim. Acta*, 2020, **362**, 137007.
21. C. L. Wang, S. Rong, Y. Q. Zhao, X. M. Wang, H. Y. Ma, *Transit. Metal Chem.*, 2021, **46**, 335-343.
22. M. Yang, S. Rong, X. M. Wang, H. Y. Ma, H. J. Pang, L. C. Tan, Y. X. Jiang, *ChemNanoMat*, 2021, **7**, 299 –306.
23. J. X. Wang, L. Zhang, L. J. Zhao, T. Li, S. B. Li, *J. Mol. Struct.*, 2021, **1231**, 129966.
24. T. Y. Li, P. He, Y. N. Dong, W. C. Chen, T. Wang, J. Gong, W. L. Chen, *Eur. J. Inorg. Chem.*, 2021, **2021**, 2063-2069.
25. Q. Q. Liu, X. L. Wang, H. Y. Lin, Z. H. Chang, Y. C. Zhang, Y. Tian, J. J. Lu, L. Yu, *Dalton T.*, 2021, **50**, 9450-9456.
26. C. X. Sun, J. Ying, Y. P. Zhang, L. Jin, A. X. Tian, X. l. Wang, *CrystEngComm*, 2022, **24**, 587-600.

27. X. Xu, Y. Q. Zhang, J. Ying, L. Jin, A. X. Tian, X. l. Wang, *CrystEngComm*, 2022, **24**, 1267-1278.
28. J. L. Zhuo, Y. L. Wang, Y. G. Wang, M. Q. Xu, J. Q. Sha, *CrystEngComm*, 2022, **24**, 579-586.
29. S. F. Ma, J. Ying, Y. P. Zhang, A. X. Tian, *CrystEngComm*, 2022, **24**, 2891-2902.